PAPER

An *in situ* DRIFTS-MS study on elucidating the role of V in the selective oxidation of methacrolein to methacrylic acid over heteropolyacid compounds†

Sarayute Chansai, [iD] *a Yuki Kato, [iD] b
Wataru Ninomiya[b] and Christopher Hardacre [iD] *a

The role of vanadium in 11-molybdo-1-vanadophosphoric acid ($H_4PMo_{11}VO_{40}$, HPMoV) has been investigated and compared with 12-modybdophosphoric acid ($H_3PMo_{12}O_{40}$, HPMo) using *in situ* diffuse reflectance infrared Fourier transform spectroscopy (DRIFTS) coupled with mass spectrometry (MS). It has been found for the first time that there are differences in the DRIFT spectra of carbonyl- and carboxylate-type species recorded in the region of 1900–1200 cm^{-1} between the two catalysts under methacrolein (MAL), MAL + O_2, and MAL + O_2 + H_2O reaction conditions at 320 °C and the MS results show faster formation of methacrylic acid over HPMoV than over HPMo catalysts. A number of hydrocarbon species adsorbed on the surface have been identified in the DRIFTS analysis including a 5-membered ring lactone-type species, a 6-membered ring lactone-type species, bidentate methacrylate species, monodentate methacrylate species, and π-adsorbed species, with the presence of V in the heteropolyacid Keggin structure favouring the formation of monodentate methacrylate surface species compared with lactone-type surface species under MAL + O_2 + H_2O reaction conditions at 320 °C. The monodentate methacrylate surface species is proposed to be the intermediate in the final step for the formation of MAA. It is likely that the same mechanism of selective oxidation of MAL occurs with and without the substitution of Mo with V, with the presence of V resulting in a faster formation of active monodentate methacrylate intermediates.

1. Introduction

Heteropolyacids (HPAs) used as oxidation catalysts have been extensively investigated for many decades[1–39] due to their acid and redox properties, high thermal stability, simple preparation procedure, and simple physical property modification such as solubility and surface areas.[3,5,7,12–16,18,20,21,26,40,41] In general, the clusters of HPAs are made up of metal–oxygen anions with different molecular sizes, compositions, and structures.[38,39] One of the HPAs that has received much attention is the Keggin-type structure with the formula $[XM_{12}O_{40}]^{n-}$, typically composed of a central XO_4 tetrahedral unit surrounded by twelve octahedrons of MO_6 units, linked by corner- and edge-sharing oxygen atoms. $[PMo_{12}O_{40}]^{3-}$ is a member of the Keggin-type HPA family,

which exhibits two defining characteristics (Brønsted acidity and redox behaviour). $H_3PMo_{12}O_{40}$ (HPMo) and its salts have been reported to show excellent catalytic oxidation of various types of hydrocarbons.[11,14,17,19,23–26,29–32,34,38,39] The selective oxidation of methacrolein (MAL) to methacrylic acid (MAA) over heteropolyacids has been extensively studied[1,4,15,26–28,30–32,35–37] since MAA is an important chemical in the production of methyl methacrylate and other derivatives including polymers.

Previous research[4,29,30,32] has shown that partially substituting Mo with V in the primary Keggin structure enhances the catalytic activity of MAL oxidation to the selective form MAA. The vanadyl species in a range of HPA catalysts were investigated for the oxidation and dehydration of methanol,[25] oxidation of isobutane[14,24,38] and isobutyric acid,[7,8,11,17] and partial oxidation of propane,[23] for example, ascertaining the role and promotional effect of V on the catalytic activity and product selectivity.

Deußer and co-workers[4] investigated the effect of V on the kinetics of catalytic MAL oxidation to MAA over various Cs_x-$H_{3+y-x}PMo_{12-y}V_yO_{40}$ catalysts. It was reported that the presence of V moderately influenced the rate of MAL oxidation but substantially decreased the rate of MAA oxidation, hence the

a Department of Chemical Engineering, Engineering Building A, The University of Manchester, Manchester M13 9PL, UK.
E-mail: sarayute.chansai@manchester.ac.uk, c.hardacre@manchester.ac.uk
b MMA Group, Monomers & Catalysts Laboratory, Mitsubishi Chemical Corporation, 20-1 Miyuki-cho, Otake-shi, Hiroshima 739-0693, Japan

† Electronic supplementary information (ESI) available. See DOI: http://doi.org/10.1039/d4cy00552j

5096 | *Catal. Sci. Technol.*, 2024, **14**, 5096–5106

This journal is © The Royal Society of Chemistry 2024

significant decrease in a consecutive oxidation of MAA and resulting in an increase in the selectivity of MAA.

Song et al.[13] studied the redox properties of several Keggin-type HPA compounds as a function of the counter-cation, heteroatom, and polyatom substitution, in which their reduction potentials were electrochemically measured. They reported that the V-substituted $H_{3+y}PMo_{12-y}V_yO_{40}$ samples demonstrated an increase in the reduction potential in comparison with the $H_3PMo_{12}O_{40}$ compound, indicative of different redox properties, which can be tuned and designed for the selective oxidation transformations.

Several studies[5,16–23,25,26] have investigated the nature of the active vanadyl species in the Keggin structure that could promote the selective oxidation reactions. It was reported[22] that heteropoly anions, $[PMo_{11}VO_{40}]^{4-}$, in the $H_4PMo_{11}VO_{40}$ catalyst were not stable during calcination and reaction, resulting in a partial decomposition and a defect of the Keggin structure. This behaviour facilitated the migration of V atoms from primary to secondary structures.

Recently, Zhou et al.[30] reported an in-depth study on vanadyl species for the oxidation of MAL to MAA over three HPA catalysts containing different vanadyl species in primary and secondary structures, i.e. $H_4PMo_{11}VO_{40}$ (V in the primary structure), $HVOPMo_{12}O_{40}$ (V in the form of VO^{2+} in the secondary structure), and $V_2O_5/H_3PMo_{12}O_{40}$ (V in the form of V_2O_5 before calcination under air). It was found that after calcination of all V-containing HPA catalysts, the vanadyl species were detected in the form of ions, resulting in a breaking of the symmetry of the Keggin structure. However, during the oxidation reaction of MAL to MAA, these independent vanadyl ions were transformed into a defective Keggin structure or a squashed square pyramidal form of the Keggin structure. They also reported that the $V_2O_5/H_3PMo_{12}O_{40}$ catalyst showed the best catalytic performance due to several active vanadyl species formed under calcination and reaction conditions. It was concluded that the vanadyl ions located in the secondary structure were transformed and interacted with the primary Keggin structure during the oxidation of MAL to MAA. Those vanadyl ions were identified as V^{4+} ions, whose amount was correlated with the selectivity of MAA.

Although the effect and properties of V in HPA catalysts[4,5,16,26,29,30] in promoting MAL conversion and MAA selectivity have been reported, the mechanistic understanding of the effect of V on the surface reaction remains unclear. In particular, infrared studies on the hydrocarbon-derived surface species under reaction conditions are very limited. In the present work, DRIFTS-MS has been used to gain a better understanding of and an insight into the role of V in the reaction mechanism during the oxidation of MAL to MAA over Keggin-type $H_3PMo_{12}O_{40}$ and $H_4PMo_{11}V_1O_{40}$ catalysts.

2. Experimental

In this study, both $H_3PMo_{12}O_{40}$ (HPMo) and $H_4PMo_{11}VO_{40}$ (HPMoV) catalysts were obtained from Mitsubishi Chemical Corporation. The catalyst was formed from hydrous 12-molybdophosphoric acid ($H_3PMo_{12}O_{40}\cdot xH_2O$, Nippon Inorganic Colour and Chemical Co., Ltd.) extracted from an aqueous solution of $H_3PMo_{12}O_{40}$ and diethyl ether. $H_3PMo_{12}O_{40}\cdot xH_2O$ was then recrystallised from an aqueous solution and the solid dried at 60 °C overnight.[36]

In situ DRIFTS measurements were performed using a Bruker Tensor 27 FTIR spectrometer equipped with a liquid N_2-cooled detector. Approximately 40 mg of catalyst sample was placed in a ceramic crucible in the in situ DRIFTS cell. The exit lines were connected to a Hiden Analytical HPR-20 mass spectrometer in order to monitor the gas phase species: H_2O ($m/z = 18$), MAL ($m/z = 70$), and MAA ($m/z = 86$).

Prior to the DRIFTS experiments, the catalyst was pretreated by heating in Ar at a total flow rate of 100 cm^3 min^{-1} ramping the temperature to 320 °C at a rate of 10 °C min^{-1}. Then the catalyst was held at this temperature for 60 min. Subsequently, the IR spectrum of the treated HPA catalyst was taken as a background.

The reactant gases used were MAL (95%, Sigma-Aldrich), O_2 (99.99% BOC), and Ar (99.99% BOC). O_2 and Ar were fed from independent Aera™ PC-7700C mass flow controllers. MAL and water vapour were introduced to the system by means of separate saturators with Ar as the carrier gas. The MAL saturator was placed in an ice water bath and the temperature of the H_2O saturator was controlled by Grant™ GD120 thermostatic baths. All the gas lines following the water and MAL saturators were trace heated to prevent condensation. The concentrations of the reactants used were 3500 ppm MAL, 7000 ppm O_2, 7000 ppm H_2O (when added), and Ar balance. The total flow rate was 100 cm^3 min^{-1}. Gas flows were carefully equilibrated using micrometer needle valves to adjust the pressure between the gas flows on each side of the four-way valve with a high-sensitivity differential pressure detector. This avoided the production of spikes on the MS signal when switching from one mixture to another.

Two different types of in-situ DRIFTS-MS experiments were carried out. The first set of experiments was designed to investigate the effect of V on the changes of surface and gas phase species under different gas feeds, i.e. MAL + Ar, MAL + O_2 + Ar and MAL + O_2 + H_2O + Ar feeds. After Ar pretreatment, the HPMo catalyst was exposed to each gas feed for 30 min at 320 °C. Our previous work[36,37] reported the important role of water in the formation of MAA, therefore, the second set of experiments was performed using H_2O switches in and out of the MAL + O_2 feed to probe the role of V. After Ar pretreatment, the HPMo catalyst was exposed to the MAL + O_2 gas feed for only 1 min at 320 °C to allow surface species to be formed and then the cycling switches of H_2O in (5 min) and out (5 min) of the MAL + O_2 + Ar feed were performed for 4 cycles.

All in situ DRIFT spectra were recorded with a resolution of 4 cm^{-1} with an accumulation of 64 scans every 30 s and the DRIFT spectra were analysed using OPUS software. The IR data are reported as $\log 1/R$ (absorbance), with $R = I/I_0$, where R is the sample reflectance, I is the intensity measured

This journal is © The Royal Society of Chemistry 2024

Catal. Sci. Technol., 2024, **14**, 5096–5106 | **5097**

under reaction conditions, and I_0 is the intensity measured on the pure HPMo sample under a flow of argon at 320 °C.

3. Results and discussion

3.1 *In situ* DRIFTS-MS and IR assignments

3.1.1 Formation of gas phase MAA. Fig. 1 shows the comparison of the evolution of gas phase MAA formation under different reaction conditions over HPMo and HPMoV catalysts at 320 °C. Fig. 1a shows that under MAL adsorption conditions, the formation of MAA on the HPMoV catalyst rises more rapidly than over HPMo. The formation of gas

Fig. 1 Comparison of the evolution of MAA formation at 320 °C as a function of time on stream over $H_3PMoO_{12}O_{40}$ and $H_4PMoO_{11}VO_{40}$ under MAL (a), MAL + O_2 (b), and MAL + O_2 + H_2O (c). The gas feed is composed of 3500 ppm MAL (when added), 7000 ppm O_2 (when added), 7000 ppm H_2O (when added), and Ar balance and the total flow rate is 100 cm³ min⁻¹.

phase MAA peaks at about 4 and 10 ppm for HPMo and HPMoV, respectively, within 3 min before decreasing slowly to zero over the course of 30 min. This behaviour is due to the depletion of surface oxygen.[12] In the presence of O_2, MAA formation does not decrease to zero and there is steady-state production as a result of the surface oxygen species being replenished, in agreement with the profile observed without the presence of O_2. Again, HPMoV was found to have a faster production of gaseous MAA than HPMo, reaching the maximum concentration at about 14 ppm in 3 min before gradually decreasing to 10 ppm over 30 min reaction on stream. In comparison, slower MAA formation was observed over HPMo before reaching the same steady-state level at 10 ppm after 10 min under the MAL + O_2 reaction feed. Thereafter, there is no significant difference in MAA formation over the two HPA samples. Similarly, the addition of H_2O into the MAL + O_2 feed (Fig. 1c) leads to a further increase in MAA production, which is more pronounced over HPMoV than over HPMo. The concentration of MAA on HPMoV reaches *ca.* 22 ppm in 2 min and then slowly decreases to 16 ppm over 30 min reaction time. These results are consistent with previous reports.[36,37]

Overall, the current work shows that there is a difference in the release of desirable gas phase MAA product from the HPMo catalyst under all three different reaction conditions compared with over the HPMoV catalyst at 320 °C. A comparison of *in situ* DRIFT spectra, recorded at 2 min under different reaction conditions and corresponding to the gaseous MAA profiles displayed in Fig. 1, is shown in Fig. 2.

3.1.2 *In situ* DRIFTS and IR assignments. In the current study, the focus of the DRIFTS study has been on the assignment and changes in IR bands appearing in the region of 2100–1200 cm⁻¹, associated with hydrocarbon-derived surface species. Fig. 2 illustrates the comparison of typical *in situ* DRIFT spectra obtained under MAL, MAL + O_2, and MAL + O_2 + H_2O reaction conditions over both HPMo and HPMoV catalysts at 320 °C. Despite the complexity of *in situ* DRIFT spectra with the rapid accumulation of surface-derived HC species between 2100 and 1200 cm⁻¹, there are three distinct areas for the IR bands at 1800–1700 cm⁻¹, 1650–1450 cm⁻¹, and below 1400 cm⁻¹. These are typically associated with carbonyl-, unsaturated double bonds and carboxylate-type species, and bending vibration of –CH groups, respectively.[9,42–47] Fig. 3 shows a schematic summary of the proposed surface species.[9,36,37,42–47]

Under MAL adsorption conditions at 320 °C (Fig. 2a), KBr was initially used as an inert and reference material. It is clearly observed that the carbonyl (C=O) group of gas-phase MAL at 1715 cm⁻¹ is the only significant IR feature, which can also be seen over both HPA catalysts. In contrast to KBr powder, several IR bands were also observed over both HPMo and HPMoV catalysts (Fig. S1 and S2,† respectively).

Considering the IR bands above 1700 cm⁻¹, in comparison with the gas phase MAL (free v(C=O), 1715 cm⁻¹), the IR band observed at 1793 cm⁻¹ would generally be associated
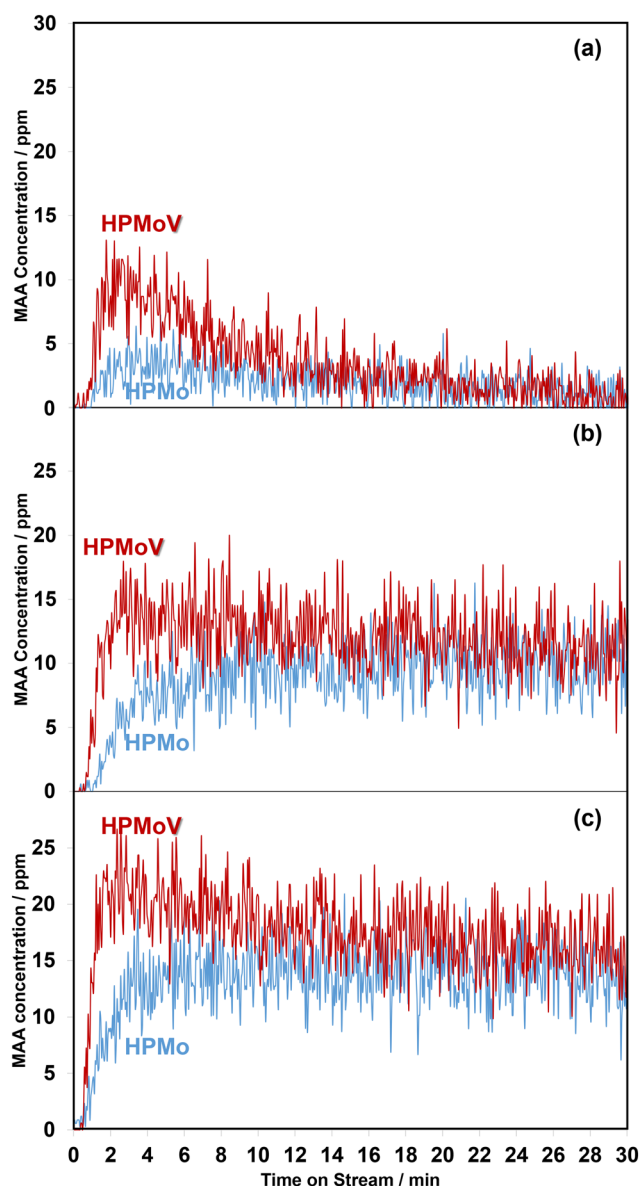
5098 | *Catal. Sci. Technol.*, 2024, **14**, 5096–5106

This journal is © The Royal Society of Chemistry 2024

Fig. 2 Comparison of *in situ* DRIFT spectra recorded at 320 °C over $H_3PMoO_{12}O_{40}$ and $H_4PMoO_{11}VO_{40}$ at 2 min under MAL (a), MAL + O_2 (b), and MAL + O_2 + H_2O (c). The gas feed is composed of 3500 ppm MAL (when added), 7000 ppm O_2 (when added), 7000 ppm H_2O (when added), and Ar balance and the total flow rate is 100 cm³ min⁻¹.
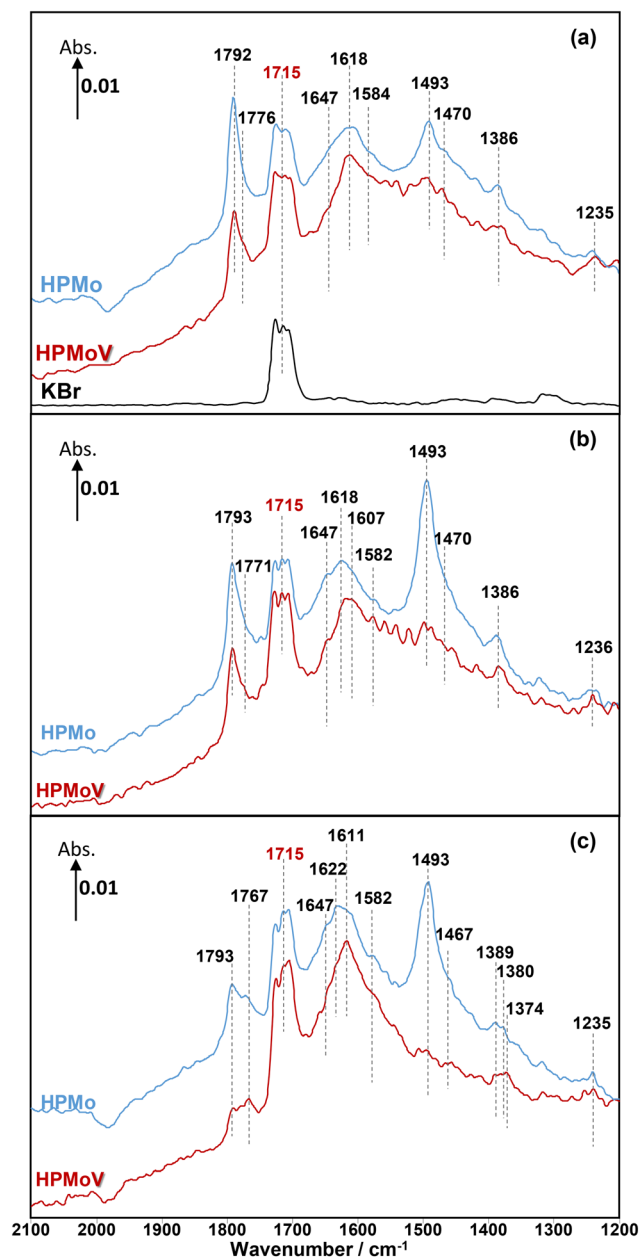
lactone formed over the HPA catalysts. However, Schaidle and co-workers[45] recently carried out DRIFTS work on the deoxygenation of acetic acid over molybdenum carbides and reported that the double IR bands at 1800–1780 cm⁻¹ are associated with symmetric and asymmetric $\nu(C=O)$ in monodentate acetates, derived from acetic acid. Our DRIFTS work has shown that the peak at 1793 cm⁻¹ appears as a single and strong IR band and is tentatively associated and assigned to the $\nu(C=O)$ group in cyclic lactone.

Fig. 2 shows IR bands at 1647 and 1618 cm⁻¹ which are attributed to the stretching vibration of unreacted carbon double bonds $\nu(C=C)$, possibly with different adsorption configurations as bidentate methacrylate adsorbed species (**Ads3**), monodentate methacrylate adsorbed species (**Ads4**), and π-adsorbed species (**Ads5**). The shoulders at 1584 and 1470 cm⁻¹ may be associated with the asymmetric and symmetric stretching vibration of carboxylate-type surface species ($\nu_{as}OCO$ and ν_sOCO), respectively. In this case, the formation of bidentate methacrylate adsorbed species (**Ads3**) shifted the vibration of the unreacted C=C bond to 1647 cm⁻¹ due to unconjugated configuration, while the carbonyl group of monodentate methacrylate adsorbed species (**Ads4**) is conjugated with the C=C bond, resulting in a slightly lower wavenumber of the C=C bond at 1618 cm⁻¹. It is important to note that the bending vibration of adsorbed and gas phase H_2O, $\delta(HOH)$, is commonly observed in the region of 1670–1570 cm⁻¹.[6,37,44] The presence of this band overlaps with the IR signal of the C=C bond at 1618 cm⁻¹ and its observation becomes increasingly challenging with H_2O accumulation on the catalyst surfaces over the course of the reaction.

Furthermore, a significantly more intense peak at 1493 cm⁻¹ was observed over HPMo compared with HPMoV. Krauß *et al.*[9] carried out DRIFTS measurements on MAL and MAA adsorptions over $Mo_9V_3W_{12}O_x$ mixed oxides as well as the $Cs_2H_2PMo_{11}VO_{40}$ heteropolyacid compound. The IR band observed at 1520–1490 cm⁻¹ was assigned to π-complex adsorption (**Ads5**) over partially reduced MoO_x. This adsorption can be facilitated by the availability of partially reduced Mo (IV and V) species. However, it is expected that fresh HPA catalysts initially possess the terminal group of $(Mo=O_t)$ in the Keggin structure, meaning that π-complex adsorption (**Ads5**) should not be substantially formed over HPA compounds. Therefore, it is likely that the IR band at 1493 cm⁻¹ is related to a carboxylate species,[42–46] for example, the bidentate methacrylate adsorbed species (**Ads3**).

In addition to MAL adsorption, the adsorption of MAA on HPMo, HPMoV, and KBr at 320 °C was carried out to help identify the surface species. As shown in Fig. 4, on KBr, a strong carbonyl vibration associated with gas phase MAA was observed, which is split into bands at 1768 and 1751 cm⁻¹ due to vibrational stretching of $\nu(C=O)$ and $\nu(C-O^-)$. At 320 °C, there is an absence of the $\nu(C=C)$ stretching band at 1632 cm⁻¹ and $\delta(CH_3)$ bending at 1386 cm⁻¹, which is consistent with the work by Krauß *et al.*[9] In contrast, over HPMo and HPMoV significant differences in the surface

with an anhydride species;[43] however, anhydrides typically consist of two IR bands due to the asymmetric and symmetric stretch of O=CO. In the present spectra, the additional higher wavenumber IR band/shoulder was not observed; this suggests that the surface species responsible for the band at 1793 cm⁻¹ is associated with the formation of cyclic lactone-type adsorbed species, for example, **Ads1** and **Ads2** in Fig. 3. This feature is at a higher wavenumber than typically found for lactone carbonyl groups (1750–1700 cm⁻¹) and the shift is likely to be due to the cyclic nature of the

This journal is © The Royal Society of Chemistry 2024

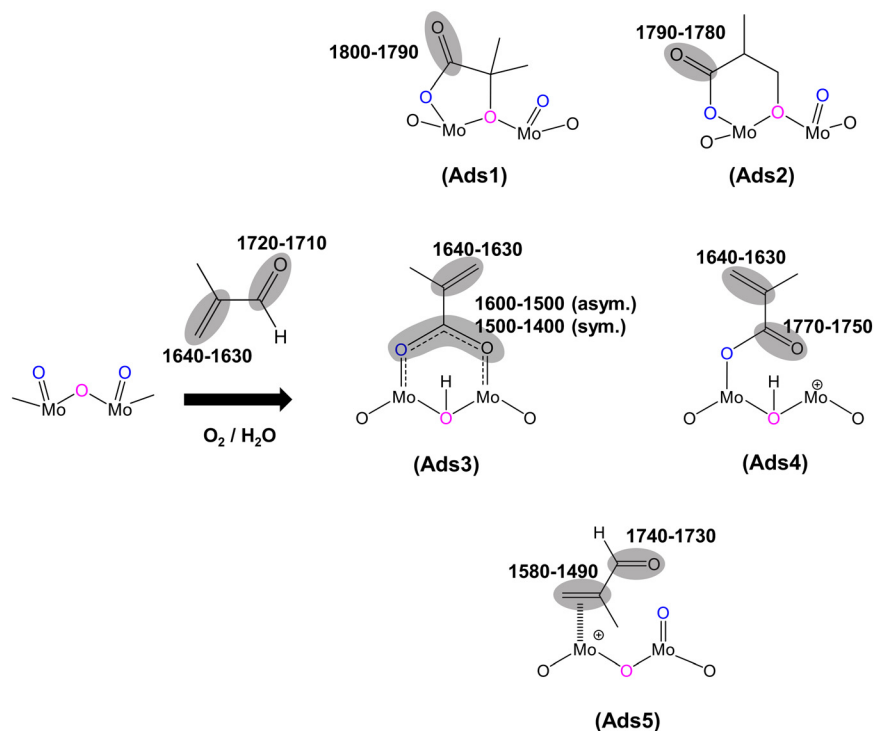*Catal. Sci. Technol.*, 2024, **14**, 5096–5106 | **5099**

Fig. 3 Proposed surface species under MAL reaction conditions at 320 °C over HPA catalysts: 5-membered ring lactone-type species (**Ads1**), 6-membered ring lactone-type species (**Ads2**), bidentate methacrylate species (**Ads3**), monodentate methacrylate species (**Ads4**), and π-adsorbed species [**Ads5**].

species compared with that over KBr were observed when MAA was adsorbed. Strong IR bands at 1795–1785 cm^{-1}, assigned to lactone-type adsorbed species (**Ads1** and **Ads2**), were detected with the stretching vibration of unreacted v(C═C) at 1632 cm^{-1}. This is also accompanied by the appearance of the IR bands at 1581, 1491, and 1470 cm^{-1}, which are associated with carboxylate-type surface

species.[42–46] Previously, on adsorption of acetic acid,[42,45,46] it was also reported that the functional group (–COOH) of acetic acid readily formed the carboxylate species as acetates (H$_3$CCOO$^-$) on catalyst surfaces with the IR region of 1560–1550 cm^{-1} for v_{as}(COO$^-$) and with the IR region of 1500–1450 cm^{-1} for v_s(COO$^-$).[42–46] Therefore, it is likely that the strong IR band at 1493–1491 cm^{-1} is associated with a bidentate methacrylate species (**Ads3**).

As well as examining MAL adsorption (Fig. 2a) at 320 °C over HPAs, MAL + O$_2$ (Fig. 2b) and MAL + O$_2$ + H$_2$O (Fig. 2c) reactions were also carried out under steady-state conditions. The similarity in IR features and adsorbed species was observed under all reaction conditions. However, the presence of H$_2$O in the reaction feed has a direct impact on the formation of monodentate methacrylate adsorbed species (**Ads4**) at around 1767 cm^{-1}, and the occurrence of a lactone-type adsorbed species (**Ads1** and **Ads2**) in the IR region of 1795–1785 cm^{-1}. It is important to point out that the IR band at 1793 cm^{-1} under MAL + O$_2$ + H$_2$O reaction conditions is less pronounced than those under MAL and MAL + O$_2$ reaction feeds, *i.e.* the formation of cyclic lactone-type surface species is hindered or converted by adding H$_2$O to another adsorbed species. It is also worth noting that both Fig. 2 and 4 show similar adsorbed surface species in the IR region of 1770–1750 cm^{-1} under MAA adsorption, MAL adsorption, and MAL + O$_2$ reaction with and without adding H$_2$O at 320 °C. Therefore, it is proposed that the observation of the IR bands between 1770 and 1750 cm^{-1} is
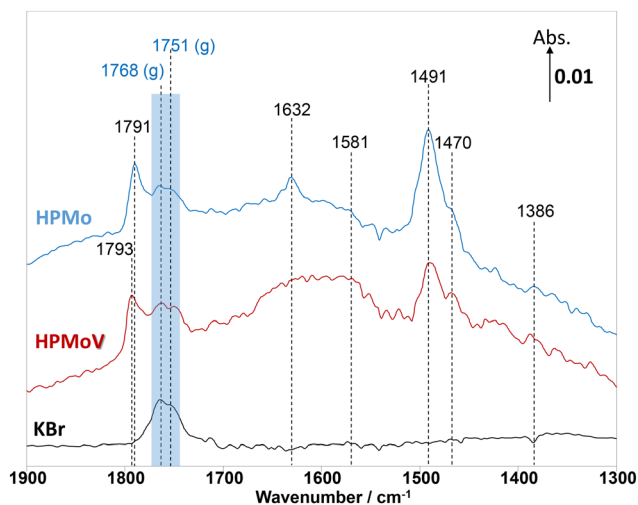

Fig. 4 Comparison of *in situ* DRIFT spectra recorded at 2 min during the adsorption of methacrylic acid (MAA) at 320 °C over H$_3$PMoO$_{12}$O$_{40}$ (HPMo), H$_4$PMoO$_{11}$VO$_{40}$ (HPMoV), The gas feed is composed of 3500 ppm MAA and Ar balance and the total flow rate is 100 cm^3 min^{-1}.

5100 | *Catal. Sci. Technol.*, 2024, **14**, 5096–5106

This journal is © The Royal Society of Chemistry 2024

associated with the stretching vibration of the $\nu(C=O)$ group of gas phase MAA or a weakly bound adsorbed MAA, possibly as monodentate methacrylate surface species (**Ads4**), which can be readily reacted and converted to form gas phase MAA.[27,32,36,37]

One important feature to be pointed out in both Fig. 2 and 4 is that bidentate methacrylate species (**Ads3**) at 1493–1491 cm^{-1} on the HPMoV catalyst is less significant than over HPMo. The presence of V in the HPMoV catalyst is thought to minimise the formation of bidentate methacrylate species (**Ads3**) but promote the formation of monodentate methacrylate adsorption (**Ads4**). Zhou et al.[30] proposed that V^{4+}/VO^{2+} species in the secondary structure rather than the primary structure has an influence on the formation and selectivity to MAA during the oxidation reaction of MAL to MAA due to the presence of accessible active vanadyl species. Bayer et al.[17] also reported higher catalytic oxidative dehydrogenation of isobutyric acid to MAA on $H_4PMo_{11}VO_{40}$ than on $H_3PMo_{12}O_{40}$ because $H_4PMo_{11}VO_{40}$ was reduced and partially decomposed, resulting in more active V^{4+} sites during the reaction.

Additional DRIFTS analysis by integrating the spectra between 1800 and 1760 cm^{-1} over the 30 min reaction period has been used to quantify the changes observed. Fig. S3† shows the comparison of changes in the ratio of monodentate methacrylate species (**Ads4**) in the IR range of 1770–1760 cm^{-1} to lactone-type adsorbed species (**Ads1** and **Ads2**) between 1800 and 1780 cm^{-1}. It is found that all ratios of monodentate methacrylate species (**Ads4**) to lactone-type surface species (**Ads1** and **Ads2**) under three different reaction conditions at 320 °C over the HPMoV catalyst change more rapidly than those over the HPMo catalyst, indicative of faster and more significant formation of monodentate methacrylate surface species (**Ads4**) on the HPMoV catalyst. Therefore, in the present work, it is likely that the reducibility of the $H_4PMo_{11}VO_{40}$ catalyst leads to the formation of these active V^{4+}/VO^{2+} species,[30] which facilitates the conversion of bidentate methacrylate species (**Ads3**) to and/or the direct formation of monodentate methacrylate surface species (**Ads4**). As a result, more MAA is formed over HPMoV than over HPMo catalysts, as shown in Fig. 1.

Recently, Tian et al.[48] reported a density functional theory (DFT) study and proposed a reaction mechanism which operated via the abstraction of proton from MAL and the formation of monodentate methacrylate species over the bridge oxygen of HPA compounds as a final step to form MAA. The DFT calculations[48] revealed the formation of monodentate methacrylate species with the lowest reaction energy for the HPMoV compound before producing MAA. In addition, the presence of V in the HPA compound was found to result in the highest reaction rate constant and lowest activation energy for the change from monodentate methacrylate surface species to gas phase MAA product. Interestingly, the in situ DRIFTS analysis reported, herein, is consistent with this simulation, indicating the importance of the formation of monodentate methacrylate adsorbed species (**Ads4**) and

the vital role of V present in the HPMoV catalyst in enhancing the formation of desirable MAA product.

In addition to gaseous MAA formation detected, gas phase CO and CO_2 were also observed, as shown in Fig. S4–S6.† HPMo was found to produce more CO and CO_2 than HPMoV; however, both catalysts show an initial transient CO and CO_2 formation within 5 min of exposure to the gas feeds. Fig. 5 shows the proposed mechanism for the formation of both CO and CO_2 under MAL adsorption (without co-fed O_2) at 320 °C. During MAL adsorption, the HPA surfaces are occupied by bidentate methacrylate adsorbed species (**Ads3**), and that the release of gaseous CO_2 from the surface leads to a partially reduced Mo species, which in turn forms the π-adsorbed species (**Ads5**).

In addition to the steady-state reaction under different reaction conditions at 320 °C, transient experiments were carried out by performing the switches of H_2O in and out of MAL + O_2 to probe the influence of V on the surface-adsorbed species.

3.2 H$_2$O transient switches

The influence of H_2O on the activity of MAL oxidation and the selectivity of MAA has been reported over HPA[2,27,28,36,37] and mixed oxide[49,50] catalysts. Recently, Yasuda et al.[36] and Chansai et al.[37] reported the role of water and its involvement in the reaction mechanism over HPMo, where the proton from water is used to form an –OH group in the MAA product. Fig. 6 shows the changes in gas phase MAA, while Fig. 7 demonstrates the evolution of IR bands in the region of 2100–1200 cm^{-1}, corresponding to Fig. 6 during the first cycles of H_2O switching in and out of the MAL + O_2 feed at 320 °C.

From Fig. 6, regardless of the HPA used, the production of MAA was promoted by adding H_2O into the MAL + O_2 gas feed and this is consistent with previous studies.[36,37] On exposure to MAL + O_2 reaction conditions for 1 min, MAA was formed at the start of the reaction before adding H_2O. However, an increase in MAA was noticeable over the course of 5 min of reaction when H_2O was added. On removing H_2O

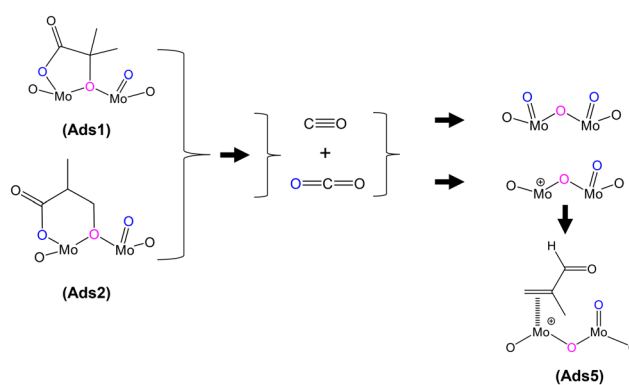**Fig. 5** Proposed formation of by-products CO and CO_2 derived from lactone-type adsorbed species during MAL adsorption at 320 °C.

This journal is © The Royal Society of Chemistry 2024

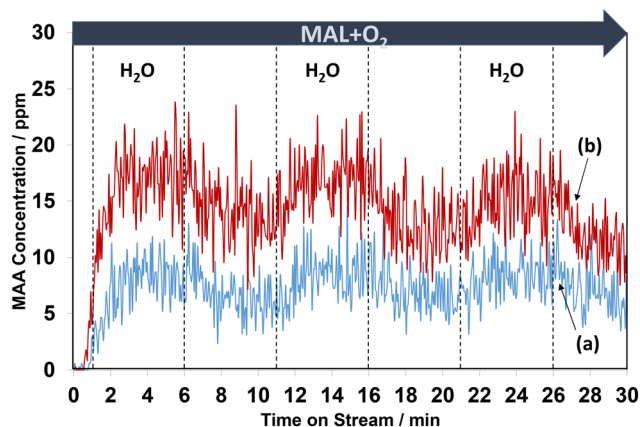Catal. Sci. Technol., 2024, **14**, 5096–5106 | **5101**

Fig. 6 Changes in gaseous MAA product as a function of time on stream at 320 °C over HPMo (a) and HPMoV (b) samples during the switches of H_2O in and out of the MAL + O_2 gas feed. The gas feed is composed of 3500 ppm MAL, 7000 ppm O_2, 7000 ppm H_2O (when added), and Ar balance and the total flow rate is 100 cm³ min⁻¹.

from the MAL + O_2 feed, a gradual decrease in the concentration of MAA was observed. Further switches of water resulted in a similar behaviour with a slow decrease in

overall concentration of MAA over the course of 30 min. As noted previously, the formation of MAA over the HPMoV catalyst was significantly higher than that over HPMo.

Fig. 7 displays the changes in *in situ* DRIFT spectra corresponding to the changes shown in Fig. 6 during the 1st cycle of H_2O switching in and out of the MAL + O_2 feed over both HPMo (Fig. 7a and b) and HPMoV (Fig. 7c and d) catalysts at 320 °C. Differences in *in situ* DRIFT spectra calculated between the H_2O switches are also provided in Fig. S7† for the comparison with Fig. 7. In Fig. 7a, over the HPMo catalyst, a significant formation of lactone-type adsorbed species (**Ads1** and **Ads2**) in the IR range of 1800–1780 cm⁻¹ was initially observed; however, on addition of H_2O to the MAL + O_2 feed, a rapid decrease in these surface species together with the bidentate methacrylate surface species (**Ads3**) at 1493 cm⁻¹ was observed. It was reported[2,49,51] that the addition of H_2O (–OH group) re-oxidised the reduced MoO_3 surfaces and this may have facilitated the decrease in those adsorbed species as a result of being transformed into more active intermediates, *i.e.* monodentate methacrylate adsorbed species (**Ads4**). It should also be noted that although the bidentate methacrylate surface species (**Ads3**) at 1493 cm⁻¹ decreased in the presence of H_2O, these species remained over the HPMo catalyst.

Fig. 7 Changes in *in situ* DRIFT spectra (2100–1200 cm⁻¹) corresponding to the formation of MAA formation shown in Fig. 3 as a function of time on stream over HPMo (a and b) and HPMoV (c and d) catalysts at 320 °C during the 2nd cycle of switches of H_2O in and out of the MAL + O_2 gas feed. The gas feed is composed of 3500 ppm MAL, 7000 ppm O_2, 7000 ppm H_2O (when added), and Ar balance and the total flow rate is 100 cm³ min⁻¹.

5102 | *Catal. Sci. Technol.*, 2024, **14**, 5096–5106

This journal is © The Royal Society of Chemistry 2024

Chansai et al.[37] reported in situ DRIFTS-MS analysis in the region of the Keggin structure between 1200 and 700 cm^{-1} during the transient H_2O/D_2O switching experiments on the HPMo catalyst at 320 °C and reported the occurrence of H–D exchange, possibly on the bridging oxygen of the Mo–O–Mo unit, where the H/D atom of water is abstracted. Therein, the H/D recombined with the monodentate carboxylate-type intermediates (proposed as monodentate methacrylate (**Ads4**) in the current work) to produce gas phase MAA. The current DRIFTS analysis shows that the formation of monodentate methacrylate species (**Ads4**) is possible and it is an important intermediate in the final step to form gaseous MAA.

When H_2O was removed from the MAL + O_2 feed in Fig. 7b, there is little change in the monodentate methacrylate species (**Ads4**) at ~1770 cm^{-1} and bidentate methacrylate adsorbed species (**Ads3**) and/or π-complex (**Ads5**) at 1495–1493 cm^{-1}. Only the surface lactone-type species (**Ads1** and **Ads2**) at 1791 cm^{-1} substantially increased due to the adsorption of MAL under MAL + O_2 reaction conditions. Once H_2O was added again, the oxidation of MAL was enhanced, resulting in an increase of carbonyl of monodentate methacrylate adsorbed species at 1770 cm^{-1}, hence facilitating the formation of gas phase MAA. It is important to point out that the accumulation of surface species under the reaction conditions is predominant on the catalyst surfaces and suppresses an observation of evident change in surface species after a couple of experimental cycles.

Similar changes to those surface species over the HPMo catalyst were observed for the HPMoV catalyst (Fig. 7c and d). In the case of the HPMoV catalyst, both adsorbed lactone-type species (**Ads1** and **Ads2**) in the IR range of 1800–1780 cm^{-1} and bidentate methacrylate species (**Ads3**) at 1493 cm^{-1} are smaller than those found over HPMo. After H_2O was removed, both adsorbed lactone-type species (**Ads1** and **Ads2**) and monodentate methacrylate species (**Ads4**) increased slightly but the bidentate methacrylate species (**Ads3**) were undetected at 1493 cm^{-1}, probably converted to monodentate methacrylate species (**Ads4**) and/or swamped by the IR signals of H_2O bending vibrations between 1670 and 1400 cm^{-1}.

Fig. 6 shows that the formation of gas phase MAA over HPMo is less than that over HPMoV; it is interesting to note from Fig. 7 that both lactone-type adsorbed species (**Ads1** and **Ads2**) at 1793 cm^{-1} and bidentate methacrylate species (**Ads3**) at 1493 cm^{-1} are evidently more pronounced over HPMo than over the HPMoV catalyst. This suggests that the formation of surface species (**Ads1**, **Ads2**, and **Ads3**) may partially block the active sites for the oxidation reaction of MAL and possibly suppress the formation of MAA to some extent. Conversely, Fig. 7 also reveals that the monodentate methacrylate adsorbed species (**Ads4**) at 1770 cm^{-1}, which is proposed to be important and associated with MAA product, is more predominant over HPMoV than over HPMo.

To gain an insight into the difference in surface species between the two HPA catalysts, the changes of the two IR ranges of 1800–1780 cm^{-1}, assigned to possibly unreactive lactone-type surface spectators (**Ads1** and **Ads2**), and of 1780–

1760 cm^{-1}, assigned to possibly active monodentate methacrylate intermediates (**Ads4**), were compared. Fig. 8 shows the comparison of the evolution of the ratio of monodentate methacrylate adsorbed species (**Ads4**) to lactone-type adsorbed species (**Ads1** and **Ads2**) during H_2O switches in and out of the MAL + O_2 feed at 320 °C. It has been found that the difference in the profile of those surface species between HPMo and HPMoV catalysts is somewhat interesting. It is clearly seen that the HPMoV catalyst demonstrates a continuous rise, while the HPMo catalyst shows both an increase and a decrease in the ratio of those species with respect to the switches of H_2O in and out of the MAL + O_2 feed over the course of 30 min.

Examining Fig. 8 between 1 and 6 min when H_2O is first introduced to the MAL + O_2 gas feed, it is found that the ratio of monodentate methacrylate adsorbed species (**Ads4**) to lactone-type adsorbed species (**Ads1** and **Ads2**) for HPMoV shows an initial rise which is slightly faster than that found for HPMo. This means that the formation of monodentate methacrylate adsorbed species (**Ads4**) is more pronounced than that of lactone-type adsorbed species (**Ads1** and **Ads2**). This suggests that the faster the formation of monodentate methacrylate surface species (**Ads4**), the more rapid the formation of gaseous MAA product, as seen in Fig. 5, where gaseous MAA is produced more significantly over HPMoV than over HPMo. Interestingly, our DRIFTS-MS analysis strongly suggests that the formation of monodentate methacrylate adsorbed species (**Ads4**) as potentially important intermediates has a significant role in facilitating the formation of gas phase MAA product.

In contrast, in the absence of H_2O between 6 and 11 min, the ratio of monodentate methacrylate adsorbed species (**Ads4**) to lactone-type adsorbed species (**Ads1** and **Ads2**) on the HPMo catalyst was decreased, indicative of a more
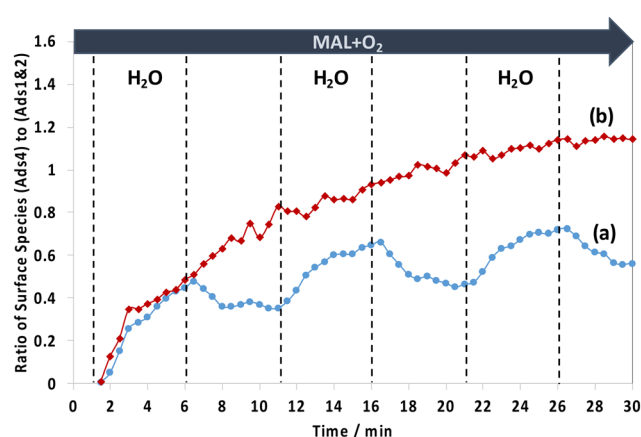

Fig. 8 Changes in the ratio of monodentate methacrylate adsorbed species (**Ads4**) in the IR range of 1780–1760 cm^{-1} to lactone-type adsorbed species (**Ads1** and **Ads2**) in the IR range of 1800–1780 cm^{-1} as a function of time on stream at 320 °C over HPMo (a) and HPMoV (b) catalysts during the switches of H_2O in and out of the MAL + O_2 feed. The gas feed is composed of 3500 ppm MAL, 7000 ppm O_2, 7000 ppm H_2O (when added), and Ar balance and the total flow rate is 100 cm^3 min^{-1}.

This journal is © The Royal Society of Chemistry 2024

Catal. Sci. Technol., 2024, **14**, 5096–5106 | **5103**

significant increase of lactone-type adsorbed species (**Ads1** and **Ads2**) than monodentate methacrylate adsorbed species (**Ads4**). It is worth noting that a different trend was observed over the HPMoV catalyst, in which the ratio of monodentate methacrylate adsorbed species (**Ads4**) to lactone-type adsorbed species (**Ads1** and **Ads2**) continues to rise, indicating that monodentate methacrylate adsorbed species (**Ads4**) are more pronounced than lactone-type adsorbed species (**Ads1** and **Ads2**). The difference in these ratios between HPMo and HPMoV catalysts suggests that the presence of V in the Keggin structure of HPA has a direct influence on the formation of monodentate methacrylate surface species (**Ads4**) rather than that of lactone-type adsorbed species (**Ads1** and **Ads2**) under reaction conditions at 320 °C.

Interestingly, there is a difference in how the surface monodentate methacrylate species (**Ads4**) change over HPMo and HPMoV catalysts, as shown in Fig. 8. The continuous rise of the ratio of monodentate methacrylate adsorbed species (**Ads4**) to lactone-type adsorbed species (**Ads1** and **Ads2**) for the HPMoV catalyst during H_2O switches in and out of the MAL + O_2 reaction over HPMoV is proposed to be due to differences in the amount of V^{4+} species present. The V $2p_{3/2}$ XPS spectra (Fig. S8†) show two vanadyl species present in the Keggin structure, i.e. V^{5+} at 517.7 eV and V^{4+} at 516.5 eV,[29,30,35] and there is a difference in the ratio of V^{4+} to V^{5+} species between both fresh and spent HPMoV catalyst, which is 0.29 and 0.82, respectively. This increase in the ratio of V^{4+} to V^{5+} species between the fresh and spent HPMoV samples after 60 min under MAL + O_2 + H_2O reaction conditions at 320 °C is consistent with the proposal that the amount of V^{4+} in HPMoV could be responsible for the formation of methacrylic acid (MAA) and the formation of monodentate methacrylate species (**Ads4**) under reaction conditions with and without H_2O. Zhou et al.[30] also reported that the amount of V^{4+} is correlated with methacrylic acid formation. This change in oxidation state of vanadyl species from V^{5+} to V^{4+} species may also explain the continuous rise of the ratio of monodentate methacrylate adsorbed species (**Ads4**) to lactone-type adsorbed species (**Ads1** and **Ads2**) for HPMoV due to (1) an increase in V^{4+}/VO^{2+} species as proposed by Zhou et al.[30] and (2) the high reaction rate constant and low activation energy to form the monodentate methacrylate species as recently reported by Tian and co-workers.[48]

Additionally, we have investigated the acid properties of both HPMo and HPMoV catalysts using in situ DRIFTS technique and pyridine adsorption at 320 °C. The comparison of in situ DRIFT spectra of pyridine adsorption at 320 °C (recorded at 10 min under Ar purge after the pyridine adsorption at 30 °C for 60 min) for both HPMo and HPMoV catalysts is shown in Fig. S9.† Interestingly, the ratio of Brønsted to Lewis acid sites on HPMoV (57.7) is much greater than that on HPMo (14.9). Consistent with this study, previous studies[52–56] were carried out to investigate the acid properties of HPA compounds and showed that strong Brønsted acid sites facilitated the activation of MAL due to

an increase in the electrophilicity of the carbonyl carbon of MAL.[55] This led to an enhancement of catalytic oxidation activity and the formation of desirable MAA product via the repulsive interaction between Brønsted sites and acidic MAA product. These Brønsted acid sites perhaps explain the observation of the present work that the HPMoV catalyst exhibits faster and more formation of active monodentate methacrylate adsorbed species (**Ads4**) to produce gas phase MAA than the HPMo catalyst as presented in Fig. 6–8.

It is important to note that the continuous rise of the ratio of monodentate methacrylate adsorbed species (**Ads4**) to lactone-type adsorbed species (**Ads1** and **Ads2**) for the HPMoV catalyst indicates that the surfaces of HPMoV can also act as a reservoir of monodentate methacrylate adsorbed species (**Ads4**). This is likely due to (1) a greater number of V^{4+}/VO^{2+} active sites as reported by Zhou and co-workers[30] that the substitution of Mo with V in the Keggin structure can increase the abundance of V^{4+}/VO^{2+} active sites, which influenced the redox property for better redox active sites through faster reduction and re-oxidation steps and somewhat had a direct relation to the catalytic activity and the selectivity of MAA, and (2) Brønsted acid sites present in the HPMoV catalyst, where both inactive and active surface species with the same chemical composition and structure detected by in situ DRIFTS are more rapidly formed than in the HPMo catalyst. Only a small portion of monodentate methacrylate adsorbed species (**Ads4**) is converted or reacted to produce MAA on the HPMoV catalyst.

4. Conclusions

The current work reports, for the first time, an in situ DRIFTS-MS analysis to gain an insight into the role and effect of V on the formation of MAA during the selective oxidation of MAL to MAA over HPA catalysts. Under different reaction conditions at 320 °C, the MS results show that the presence of V in the HPMoV catalyst yields higher formation of gas phase MAA product than that in the HPMo catalyst. Simultaneously, the in situ DRIFTS analysis reveals that several possible HC-adsorbed species have been formed and tentatively identified: a 5-membered ring lactone-type species (**Ads1**), a 6-membered ring lactone-type species (**Ads2**), bidentate methacrylate species (**Ads3**), monodentate methacrylate species (**Ads4**), and π-adsorbed MAL species (**Ads5**). Interestingly, the transient switching of H_2O in and out of the MAL + O_2 gas feed reveals that the substitution of Mo with V in the Keggin primary structure selectively and substantially facilitates the formation of monodentate methacrylate adsorbed species (**Ads4**) in the final step before forming gas phase MAA. It is important to point out that the current work reports the influence of V in the HPMoV catalyst on the surface adsorbed species under various reaction conditions in comparison with the HPMo catalyst. However, the reaction mechanism of MAL to MAA between the two catalysts is not differentiated. It is likely that the same mechanism of selective oxidation of MAL

5104 | Catal. Sci. Technol., 2024, **14**, 5096–5106

This journal is © The Royal Society of Chemistry 2024

occurs but in the presence of V in the Keggin primary structure, the HPMoV catalyst facilitates an increased formation of reactive monodentate methacrylate intermediates (**Ads4**), resulting in further enhancement of gaseous MAA formation when compared with the HPMo catalyst.

Data availability

The data supporting this article have been included as part of the ESI.†

Conflicts of interest

There are no conflicts to declare.

Acknowledgements

References

1 Y. Konishi, K. Sakata, M. Misono and Y. Yoneda, *J. Catal.*, 1982, **77**, 169–179.

2 V. Ernst, Y. Barbaux and P. Courtine, *Catal. Today*, 1987, **1**, 167–180.

3 K. Eguchi, T. Seiyama, N. Yamazoe, S. Katsuki and H. Taketa, *J. Catal.*, 1988, **111**, 336–344.

4 L. M. Deußer, J. W. Gaube, F.-G. Martin and H. Hibst, in *11th International Congress On Catalysis - 40th Anniversary*, ed. J. W. Hightower, W. Nicholas Delgass, E. Iglesia, A. T. B. T. Bell in S. S. and C., Elsevier, 1996, vol. 101, pp. 981–990.

5 K. Inumaru, A. Ono, H. Kubo and M. Misono, *J. Chem. Soc., Faraday Trans.*, 1998, **94**, 1765–1770.

6 A. M. Herring and R. L. McCormick, *J. Phys. Chem. B*, 1998, **102**, 3175–3184.

7 C. Marchal-Roch, N. Laronze, N. Guillou, A. Tézé and G. Hervé, *Appl. Catal., A*, 2000, **199**, 33–44.

8 C. Marchal-Roch, N. Laronze, N. Guillou, A. Tézé and G. Hervé, *Appl. Catal., A*, 2000, **203**, 143–150.

9 K. Krauß, A. Drochner, M. Fehlings, J. Kunert and H. Vogel, *J. Mol. Catal. A: Chem.*, 2000, **162**, 413–422.

10 S. Ganapathy, M. Fournier, J. F. Paul, L. Delevoye, M. Guelton and J. P. Amoureux, *J. Am. Chem. Soc.*, 2002, **124**, 7821–7828.

11 C. Marchal-Roch, N. Laronze, R. Villanneau, N. Guillou, A. Tézé and G. Hervé, *J. Catal.*, 2000, **190**, 173–181.

12 M. Misono, *Chem. Commun.*, 2001, 1141–1152.

13 I. K. Song and M. A. Barteau, *J. Mol. Catal. A: Chem.*, 2004, **212**, 229–236.

14 N. Ballarini, F. Candiracci, F. Cavani, H. Degrand, J.-L. Dubois, G. Lucarelli, M. Margotti, A. Patinet, A. Pigamo and F. Trifirò, *Appl. Catal., A*, 2007, **325**, 263–269.

15 H. Kim, J. C. Jung, S. H. Yeom, K.-Y. Lee and I. K. Song, *J. Mol. Catal. A: Chem.*, 2006, **248**, 21–25.

16 H. Kim, J. C. Jung, D. R. Park, S.-H. Baeck and I. K. Song, *Appl. Catal., A*, 2007, **320**, 159–165.

17 R. Bayer, C. Marchal-Roch, F. X. Liu, A. Tézé and G. Hervé, *J. Mol. Catal. A: Chem.*, 1996, **114**, 277–286.

18 V. F. Odyakov, E. G. Zhizhina and K. I. Matveev, *J. Mol. Catal. A: Chem.*, 2000, **158**, 453–456.

19 P. Villabrille, G. Romanelli, P. Vázquez and C. Cáceres, *Appl. Catal., A*, 2004, **270**, 101–111.

20 G. Mestl, T. Ilkenhans, D. Spielbauer, M. Dieterle, O. Timpe, J. Kröhnert, F. Jentoft, H. Knözinger and R. Schlögl, *Appl. Catal., A*, 2001, **210**, 13–34.

21 C. Marchal-Roch, C. Julien, J. F. Moisan, N. Leclerc-Laronze, F. X. Liu and G. Hervé, *Appl. Catal., A*, 2004, **278**, 123–131.

22 T. Ressler, O. Timpe, F. Girgsdies, J. Wienold and T. Neisius, *J. Catal.*, 2005, **231**, 279–291.

23 X.-K. Li, J. Zhao, W.-J. Ji, Z.-B. Zhang, Y. Chen, C.-T. Au, S. Han and H. Hibst, *J. Catal.*, 2006, **237**, 58–66.

24 A. Brückner, G. Scholz, D. Heidemann, M. Schneider, D. Herein, U. Bentrup and M. Kant, *J. Catal.*, 2007, **245**, 369–380.

25 J. E. Molinari, L. Nakka, T. Kim and I. E. Wachs, *ACS Catal.*, 2011, **1**, 1536–1548.

26 Y.-L. Cao, L. Wang, L.-L. Zhou, G.-J. Zhang, B.-H. Xu and S.-J. Zhang, *Ind. Eng. Chem. Res.*, 2017, **56**, 653–664.

27 M. Kanno, T. Yasukawa, W. Ninomiya, K. Ooyachi and Y. Kamiya, *J. Catal.*, 2010, **273**, 1–8.

28 M. Kanno, Y. Miura, T. Yasukawa, T. Hasegawa, W. Ninomiya, K. Ooyachi, H. Imai, T. Tatsumi and Y. Kamiya, *Catal. Commun.*, 2011, **13**, 59–62.

29 F. Jing, B. Katryniok, F. Dumeignil, E. Bordes-Richard and S. Paul, *J. Catal.*, 2014, **309**, 121–135.

30 L. Zhou, L. Wang, S. Zhang, R. Yan and Y. Diao, *J. Catal.*, 2015, **329**, 431–440.

31 L. Zhou, L. Wang, Y. Cao, Y. Diao, R. Yan and S. Zhang, *Mol. Catal.*, 2017, **438**, 47–54.

32 Y.-L. L. Cao, L. Wang, B.-H. H. Xu and S.-J. J. Zhang, *Chem. Eng. J.*, 2018, **334**, 1657–1667.

33 Y. Geng, S. Xiong, B. Li, Y. Liao, X. Xiao and S. Yang, *Ind. Eng. Chem. Res.*, 2018, **57**, 856–866.

34 X. Li, J. Zhang, F. Zhou, Y. Wang, X. Yuan and H. Wang, *Mol. Catal.*, 2018, **452**, 93–99.

35 L. Zhou, S. Zhang, Z. Li, J. Scott, Z. Zhang, R. Liu and J. Yun, *RSC Adv.*, 2019, **9**, 34065–34075.

36 S. Yasuda, J. Hirata, M. Kanno, W. Ninomiya, R. Otomo and Y. Kamiya, *Appl. Catal., A*, 2019, **570**, 164–172.

37 S. Chansai, Y. Kato, W. Ninomiya and C. Hardacre, *Faraday Discuss.*, 2021, **229**, 443–457.

38 L. Zhang, S. Paul, F. Dumeignil and B. Katryniok, *Catalysts*, 2021, **11**, 769.

39 M. J. da Silva, A. A. Rodrigues and N. P. G. Lopes, *Inorganics*, 2023, **11**, 162.

40 M. Misono, K. Sakata, Y. Yoneda and W. Y. Lee, in *Studies in Surface Science and Catalysis*, ed. T. Seiyama and K. Tanabe, Elsevier, 1981, vol. 7, pp. 1047–1059.

41 N. Essayem, G. Coudurier, M. Fournier and J. C. Védrine, *Catal. Lett.*, 1995, **34**, 223–235.

This journal is © The Royal Society of Chemistry 2024

Catal. Sci. Technol., 2024, **14**, 5096–5106 | 5105

42 W. Rachmady and M. A. Vannice, *J. Catal.*, 2002, **208**, 170–179.

43 S. Kohl, A. Drochner and H. Vogel, *Catal. Today*, 2010, **150**, 67–70.

44 G. Y. Popova, Y. A. Chesalov, E. M. Sadovskaya and T. V. Andrushkevich, *J. Mol. Catal. A: Chem.*, 2012, **357**, 148–153.

45 J. A. Schaidle, J. Blackburn, C. A. Farberow, C. Nash, K. X. Steirer, J. Clark, D. J. Robichaud and D. A. Ruddy, *ACS Catal.*, 2016, **6**, 1181–1197.

46 M. Zhou, H. Zhang, H. Ma and W. Ying, *Fuel Process. Technol.*, 2016, **144**, 115–123.

47 H. Alalwan and A. Alminshid, *Spectrochim. Acta, Part A*, 2020, **229**, 117990.

48 Y. Tian, H. Yan, J. Li, Y. Yang, T. Guo, X. Zhang, S. Xiang and C. Li, *Ind. Eng. Chem. Res.*, 2024, **63**, 4807–4816.

49 H. Böhnke, J. Gaube and J. Petzoldt, *Ind. Eng. Chem. Res.*, 2006, **45**, 8794–8800.

50 H. Böhnke, J. Gaube and J. Petzoldt, *Ind. Eng. Chem. Res.*, 2006, **45**, 8801–8806.

51 S. Kwon, P. Deshlahra and E. Iglesia, *J. Catal.*, 2018, **364**, 228–247.

52 I. K. Song, M. S. Kaba and M. A. Barteau, *J. Phys. Chem.*, 1996, **100**, 17528–17534.

53 M. J. Janik, R. J. Davis and M. Neurock, *Catal. Today*, 2005, **105**, 134–143.

54 A. M. Alsalme, P. V. Wiper, Y. Z. Khimyak, E. F. Kozhevnikova and I. V. Kozhevnikov, *J. Catal.*, 2010, **276**, 181–189.

55 S. Yasuda, A. Iwakura, J. Hirata, M. Kanno, W. Ninomiya, R. Otomo and Y. Kamiya, *Catal. Commun.*, 2019, **125**, 43–47.

56 C. Pezzotta, V. S. Marakatti and E. M. Gaigneaux, *Catal. Sci. Technol.*, 2020, **10**, 7984–7997.

5106 | *Catal. Sci. Technol.*, 2024, **14**, 5096–5106

This journal is © The Royal Society of Chemistry 2024